Joint user activity detection, channel estimation and decoding for multi-user/multi-antenna OFDM systems

Frederic Lehmann

***Abstract*—We propose a Bayesian framework for the problem of multi-user dectection in the context of an unknown and time-varying number of active users. In this paper, we combine orthogonal frequency-division multiplexing modulation with multi-antenna reception to mitigate both the asynchronism and frequency-selectivity of the wireless medium. We develop a method for user identity and data detection with joint channel parameter estimation, performed on a per-OFDM block basis to account for a highly dynamic random-access channel. Based on a factor graph approach, we derive an inference algorithm based on message-passing resulting in an iterative code-aided receiver. We show that a suitable Gaussian approximation leads to a complexity that increases only linearly with the maximum number of users.**

Computer simulations show that the proposed iterative receiver has a low probability of erroneous activity detection, while maintaining a high antenna diversity order for active users.

***Index Terms*—Multi-antenna OFDM, multi-user detection, user activity detection, channel estimation, graphical models, message-passing receiver.**

I. Introduction

Future mobile and wireless communications networks will require unprecedented levels of energy and spectrum efficiency. Here, we list some of the key technologies able to meet these challenging goals. First, traffic offloading using unlicensed frequency bands [1] can opportunistically utilize spectral holes, provided that the presence/absence of primary users is correctly detected. Secondly, decode-and-forward relaying [2] extends the radio coverage by taking advantage of cooperative diversity. However, since the destination experiences error propagation if a decoding error at the relay is not considered, the destination may need to detect which codeword was properly decoded and reforwarded by which relay. Thirdly, Internet-of-Things (IoT) applications with massive connectivity and low latency requirements need uplink users to transmit their sporadic data to a base station (BS) which has no prior knowledge of the active user set [18], in order to avoid the large signaling overhead due to protocol-based user identification. What these three techniques have in common is that they need to perform user (or relay) activity detection along with data detection, which is the problem we address in this paper.

We focus on the simultaneous transmission of an unknown and time-varying number of single-antenna users employing orthogonal frequency-division multiplexing (OFDM) whose asynchronism is compensated by long-enough cyclic-prefixes (CPs), combined with receiver diversity to combat multipath fading over wireless channels.

Several user activity detection (UAD) and multi-user detection (MUD) algorithms suitable for multi-antenna OFDM systems have been investigated in the literature.

Standard approaches implement active user set detection and MUD as separate modules. In the single-user case, energy detection [3], which is often the preferred user activity dectection method due to its simplicity, has been extended to multi-antenna OFDM in [4]. The obvious drawback of constant false alarm rate (CFAR) energy thresholding is its inability to deliver reliability information about user detection for the current OFDM block. Once the single user is detected, joint channel estimation, symbol detection and decoding methods, such as [5]-[6], can be applied. In the multi-user case, user-specific signatures are first sent on the multiple-access channel for the sake of user identification using CFAR techniques [7]-[8]. Then for subsequent user data, known-channel joint MUD and decoding [9] can be performed based on the channel estimates obtained during the user identification phase if the channels are quasi-static. Otherwise, either blind channel estimation [10] or joint channel estimation, MUD and decoding (CEMUDD) methods will be needed over time-varying channels [11]-[12]. Alternatively, in the context of multicarrier code-division multiple-access (MC-CDMA), a subspace method was introduced in [16] to estimate the set of active users along with the multiple-antenna channel at the receiver side. Minimum mean square error (MMSE) MUD is then applied to recover the symbols sent by the detected users.

Against this background, joint user activity and data detection, using compressive sensing [17]-[19] or serial interference cancellation (SIC) [20], appeared recently. However, these methods consider perfect channel knowledge even for inactive users, which implicitly assumes quasi-static channels that are periodically re-estimated by the transmission of beacons [20].

In this work, we propose an OFDM-based superposition modulation allowing multiple users to share the same time and frequency resources. User separation is achieved with the help of user-specific interleavers at the transmitter side [9]. We consider the challenging scenario, where the set of active users

F. Lehmann is with SAMOVAR, Télécom SudParis, CNRS, Université Paris-Saclay, 9 rue Charles Fourier 91011 EVRY, France (e-mail: frederic.lehmann@it-sudparis.eu).

Phone: (+33) 1 60 76 46 33. Fax: (+33) 1 60 76 44 33

Manuscript received March 26, 2018, revised May 14, 2018.

and the propagation parameters can vary on a per-OFDM block basis. Since users join and leave the network without prior knowledge on arrival/disappearance times, we model the per-user activity as a binary random variable. We also introduce a Gauss-Markov state-space model for the per-user multi-antenna channel frequency response (CFR) and an observation model for the received baseband signal. Bayesian inference for the resulting mixed discrete-continuous problem is then reformulated using a graphical model approach [21]-[22]. We discuss how belief propagation naturally results in an iterative joint UAD-CEMUDD scheme. However, standard message-passing involves a Gaussian mixture representation, whose number of mixands grows as a function of the subcarrier and iteration indices. As a remedy, we introduce suitable approximations to obtain a Gaussian belief propagation [23]-[24] implementation for specific parts of the receiver, leading to a tractable complexity, while preserving near-optimal performances.

The main technical contributions of this work are

- A beaconless user identification and channel acquisition protocol, suitable for delay-sensitive applications where transmissions may occur or cease at any OFDM block
- An iterative message-passing receiver performing joint UAD-CEMUDD, with a complexity that increases only linearly with the maximum number of users in the network
- A receiver that exchanges soft information not only about the transmitted data as usual, but also about the activity of each user, hence limiting the risk of error propagation during subsequent iterations.

Therefore, unlike existing OFDM-based CEMUDD [11]-[14], the present work focuses on the automatic user activity tracking and situations where the quasi-static channel assumption does not hold. Another distinctive feature of the proposed method is its ability to explicitly exploit the residual channel, symbol and user activity uncertainties in the iterative process, while existing OFDM-based CEMUDD ignore all or part of that information [11]-[15].

Throughout the paper, bold letters indicate vectors and matrices while $\mathbf{0}_{m\times n}$ (resp. $\mathbf{I}_m$) is the $m \times n$ all-zero (resp. the $m \times m$ identity) matrix and $\mathrm{diag}\{\mathbf{a}\}$ is the diagonal matrix, whose diagonal entries are stored in vector $\mathbf{a}$ and whose off-diagonal entries are zero. $\mathcal{N}_{\mathcal{C}}(\mathbf{x} : \mathbf{m}, \mathbf{P})$ denotes a complex Gaussian distribution of the variable $\mathbf{x}$, with mean $\mathbf{m}$ and covariance matrix $\mathbf{P}$. Let $\mathbf{y}_n$ be the n-th observation, $n = 1, \ldots, N$, a set of observations from time i up to time t is denoted by $\mathbf{y}_{i:t}$. The conditional expectation or covariance of a variable at time n given $\mathbf{y}_{1:n-1}$, (resp. $\mathbf{y}_{n+1:N}$) is denoted using the subscript $n|n-1$ (resp. $n|n+1:N$). Similarly, the conditional expectation or covariance of a variable at time n given $\{\mathbf{y}_1, \ldots, \mathbf{y}_{n-1}, \mathbf{y}_{n+1}, \ldots, \mathbf{y}_N\}$ is denoted using the subscript $n \setminus n$.

This paper is organized as follows. First, Sec. II describes the system model adopted for the time-varying multiple-access problem, along with the corresponding factor graph representation. In Sec. III we develop our joint user activity detection, channel estimation, MUD and decoding algorithm (joint UAD-CEMUDD) based on belief propagation over the factor graph. In Sec. IV, a low-complexity receiver based on approximate Gaussian message-passing is derived. Finally, in Sec. V, the performances of the proposed algorithm are assessed through numerical simulations and compared with existing methods.

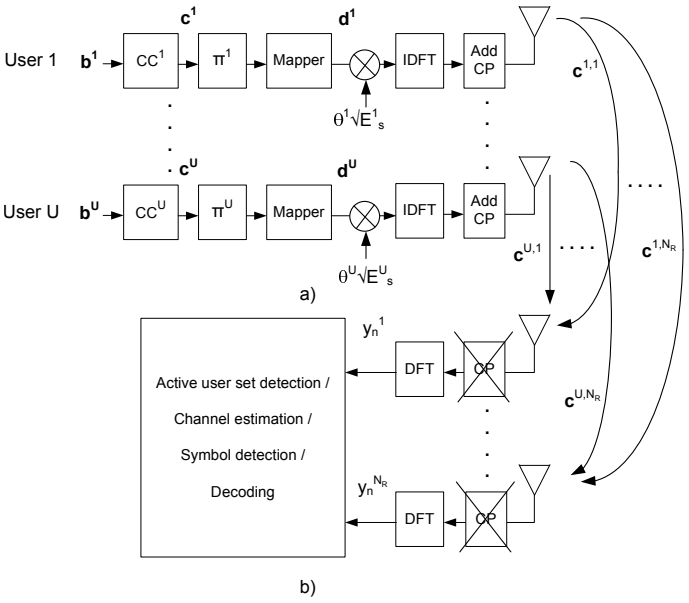

Fig. 1. a) Single-antenna OFDM transmitter for each user - b) Multi-user/multi-antenna OFDM receiver at the destination node.

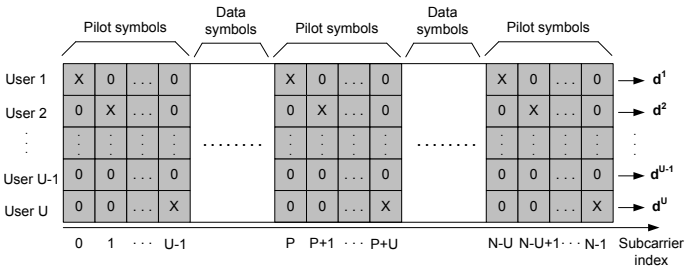

Fig. 2. Subcarrier arrangement for all users: pilot block (shaded) and data block (unshaded). In a pilot block, a 0 denotes an always silent subcarrier, while x is a pilot (resp. a silent) subcarrier for an active (resp. inactive) user.

II. System model

A. Multiple-access system

We consider the problem illustrated in Fig. 1, consisting of U single-antenna user nodes and one destination node equipped with N_R receive antennas. User u generates a sequence of uniformly, identically and independently distributed (i.i.d.) information bits, $\mathbf{b}^u$, that is encoded by the convolutional code CC^u, passed through a user-specific bit interleaver π^u and mapped into complex symbols using an M-ary modulation scheme. As illustrated in Fig. 2, orthogonal pilot sequences are inserted with repetition period P for the purpose of channel estimation. The resulting length-N modulated vector for user u is denoted by $\mathbf{d}^u = [d_0^u, d_1^u, \ldots, d_{N-1}^u]^T$, with the normalization $E[|d_n^u|^2] = 1\ \forall n$. We use the notation $\mathbf{d}^u = \mathcal{C}^u(\mathbf{b}^u)$, where $\mathcal{C}^u$ denotes the deterministic transformation corresponding to the combined effect of channel

coding, bit interleaving, mapping and pilot insertion for user u. The u-th user activity is modeled by multiplying the current modulated vector with $\sqrt{E_s^u}\theta^u$, where E_s^u is the energy per symbol of user u and θ^u a binary existence variable, that equals 1 (resp. 0) if user u is active (resp. inactive). Active users form a subset, whose size is assumed lower or equal to N_R, thus rendering the degree of freedom of the receiver sufficient. Each user implements OFDM transmission using an N-point inverse discrete Fourier transform (IDFT), in order to enable simple and effective mitigation of multipath fading at the receiver side. For convenience, the OFDM block index is dropped since we assume user appearance/disappearance as well as channel time variation on a per-OFDM block basis. We further assume that the channel length augmented by the users' maximum timing misalignment remains within the cyclic prefix (CP), so that the effect of user asynchronism at the destination is suppressed [25].

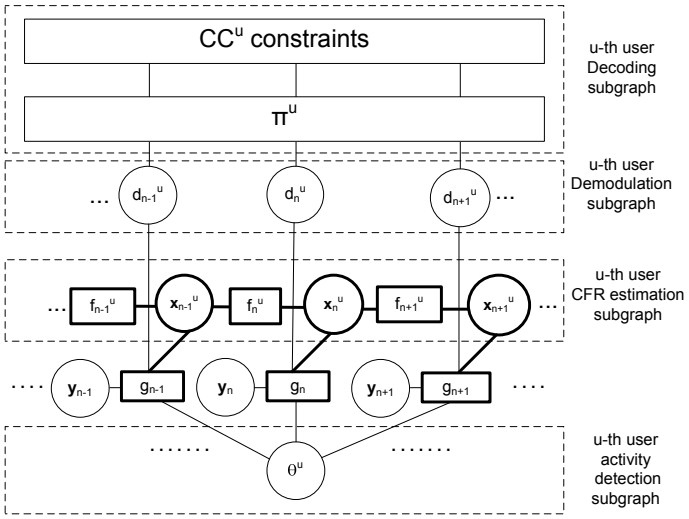

Fig. 3. Portion of the factor graph corresponding to receiver processing at the destination node for the u-th user.

B. Channel model

Assuming a block fading channel, the discrete-time channel impulse response (CIR) between user u and the m-th receive antenna is a length-L complex vector, $\mathbf{c}^{u,m} = [c^{u,m}(0), \ldots, c^{u,m}(L-1)]^T$, constant over one OFDM block. Under the wide-sense stationary uncorrelated scattering (WSSUS) model [26], the coefficients $c^{u,m}(l)$ are independently drawn from $\mathcal{N}_C(c^{u,m}(l) : 0, E\left[|c^{u,m}(l)|^2\right])$, where the normalization $\sum_{l=0}^{L-1} E\left[|c^{u,m}(l)|^2\right] = 1$ applies. It follows that the channel frequency response (CFR) between user u and the m-th receive antenna, $\{C_n^{u,m}\}_{n=0}^{N-1}$, is the N-point discrete Fourier transform (DFT) of the zero-padded CIR $\mathbf{c}^{u,m}$. Now, let us define the CFR state between user u and the destination over subcarrier n as

$$\mathbf{x}_n^u = \left[C_n^{u,1}, C_n^{u,2} \ldots, C_n^{u,N_R}\right]^T, \tag{1}$$

whose prior distribution is

$$p(\mathbf{x}_n^u) = \mathcal{N}_C(\mathbf{x}_n^u : \mathbf{0}_{N_R \times 1}, \mathbf{I}_{N_R}). \tag{2}$$

In order to get a simple factor graph representation, we model the channel frequency correlation as in [6], with a Gauss-Markov process of the form

$$\mathbf{x}_n^u = \mathbf{x}_{n-1}^u + \mathbf{\Delta}_n^u \tag{3}$$

whose i.i.d. Gaussian driving noise $\mathbf{\Delta}_n^u \sim \mathcal{N}_C(\mathbf{\Delta}_n^u : \mathbf{0}_{N_R \times 1}, \mathbf{Q}^u)$ has covariance

$$\mathbf{Q}^u = \zeta \times \operatorname{diag}\left\{\left[E[|C_n^{u,1} - C_{n-1}^{u,1}|^2], \ldots, E[|C_n^{u,N_R} - C_{n-1}^{u,N_R}|^2]\right]\right\},$$

where ζ is a real positive parameter to be optimized to account for the model inaccuracy.

C. Observation model

In the following, using the fact that subcarrier orthogonality is preserved (see Sec. II-A-II-B), we obtain the baseband signal at the m-th receive antenna on the n-th subcarrier as [10]-[12]

$$y_n^m = \sum_{u=1}^{U} \theta^u \sqrt{E_s^u} d_n^u C_n^{u,m} + w_n^m, \tag{4}$$

where $w_n^m \sim \mathcal{N}_C(w_n^m : 0, N_0)$ denotes the zero-mean i.i.d. additive white Gaussian noise (AWGN) term. Let us define the received observation vector for all receive antennas on the n-th subcarrier as $\mathbf{y}_n = [y_n^1, \ldots, y_n^{N_R}]^T$, (4) leads to

$$\mathbf{y}_n = \sum_{u=1}^{U} \theta^u \mathbf{H}_n^u(d_n^u)\mathbf{x}_n^u + \mathbf{w}_n, \tag{5}$$

where $\mathbf{H}_n^u(d_n^u) = \operatorname{diag}\left\{\left[\sqrt{E_s^u} d_n^u, \ldots, \sqrt{E_s^u} d_n^u\right]\right\}$ is the u-th user $N_R \times N_R$ observation matrix and $\mathbf{w}_n = [w_n^1, \ldots, w_n^{N_R}]^T$ is a zero-mean Gaussian noise vector with covariance matrix $\mathbf{R} = N_0 \mathbf{I}_{N_R}$.

D. Factor-graph framework

A factor-graph is a graphical representation of the factorization of a global function into a product of local functions depending on a subset of the variables [21]-[22]. Here, since Bayesian inference is of interest, the global function is the *a posteriori* probability density function (p.d.f.) of the problem at hand, whose unobserved variables correspond to all users' data or CFR variables introduced in Sec. II-A-II-B) and whose observed variables are defined in Sec. II-C. Exploiting all conditional independencies encoded by the factor-graph, Bayesian inference can then be performed in a computationally efficient manner by applying the sum-product algorithm (SPA) [21]-[22]. Let us define the u-th user CFR state variables for all subcarriers in Sec. II-B as $\mathbf{X}^u = \{\mathbf{x}_n^u\}_{n=0}^{N-1}$. Similarly, we collect the observations for all subcarriers in Sec. II-C into $\mathbf{Y} = \{\mathbf{y}_n\}_{n=0}^{N-1}$. Then, the *a posteriori* p.d.f. of interest can

be factorized using Bayes rule as

$$\begin{aligned} &p(\theta^1,\ldots,\theta^U,\mathbf{X}^1,\ldots,\mathbf{X}^U,\mathbf{d}^1,\ldots,\mathbf{d}^U,\mathbf{b}^1,\ldots,\mathbf{b}^U|\mathbf{Y}) \\ &\propto p(\mathbf{Y}|\theta^1,\ldots,\theta^U,\mathbf{X}^1,\ldots,\mathbf{X}^U,\mathbf{d}^1,\ldots,\mathbf{d}^U) \\ &\quad\times\prod_{u=1}^{U}\left\{P(\theta^u)p(\mathbf{X}^u)P(\mathbf{d}^u|\mathbf{b}^u)P(\mathbf{b}^u)\right\}, \end{aligned} \tag{6}$$

where we have introduced the reasonable assumption that user existence variables are independent of the data and CFR states. Now, using the fact that the noise vectors in (5) are i.i.d., the second line in (6) can be further factorized as

$$\begin{aligned} &p(\mathbf{Y}|\theta^1,\ldots,\theta^U,\mathbf{X}^1,\ldots,\mathbf{X}^U,\mathbf{d}^1,\ldots,\mathbf{d}^U) \\ &=\prod_{n=0}^{N-1}p(\mathbf{y}_n|\theta^1,\ldots,\theta^U,\mathbf{x}_n^1,\ldots,\mathbf{x}_n^U,d_n^1,\ldots,d_n^U). \end{aligned}$$

Moreover $\forall u$, using the deterministic relationship between $\mathbf{d}^u$ and $\mathbf{b}^u$ from Sec. II-A and the first-order Gauss-Markov model for $\mathbf{X}^u$ from Sec. II-B, the third line in (6) is proportional to

$$\prod_{u=1}^{U}\left\{P(\theta^u)I(\mathbf{d}^u=\mathcal{C}^u(\mathbf{b}^u))p(\mathbf{x}_0^u)\prod_{n=1}^{N-1}p(\mathbf{x}_n^u|\mathbf{x}_{n-1}^u)\right\},$$

where we have used the fact that $\forall u$, $P(\mathbf{b}^u)$ is an irrelevant constant and $I(.)$ denotes the indicator function. The factor-graph corresponding to the above factorization is depicted in Fig. 3. Variable nodes are represented as circles and the local functions corresponding to the n-th subcarrier in the factorization, denoted by

$$\begin{aligned} f_n^u &= p(\mathbf{x}_n^u|\mathbf{x}_{n-1}^u) \\ g_n &= p(\mathbf{y}_n|\theta^1,\ldots,\theta^U,\mathbf{x}_n^1,\ldots,\mathbf{x}_n^U,d_n^1,\ldots,d_n^U) \end{aligned}$$

are represented as squares. For the sake of readability, we have only depicted the dependencies of g_n on the user activity, data and CFR states of the u-th user. Therefore it is understood that the dependencies of g_n on the user activity, data and CFR states of all other users have exactly the same structure and should be stacked on top of each other in parallel planes in the factor graph. Note that the overall factor graph can be decomposed into a number of subgraphs, that correspond to multi-user detection tasks (such as per-user CFR estimation, soft demodulation and soft decoding), augmented by an additional UAD subgraph.

III. Belief propagation receiver

In this section we introduce a receiver, which attempts joint UAD-CEMUDD for all users. We seek a probabilistic approach computing marginals for all users' existence, data and CFR states. An efficient algorithm for computing these marginals is by iteratively passing messages among neighboring nodes on the graph in Fig. 3 via the sum-product algorithm [21]-[22]. In this section, we present the exact form of the messages exchanged over each subgraph. We let $\mu_{u\to v}(.)$ denote the message sent by node u to node v in the factor graph.

A. u-th user CFR estimation subgraph

The incoming message on the u-th user CFR estimation subgraph on to $\mathbf{x}_n^u$ is computed from the sum-product rule applied at the factor node g_n

$$\begin{aligned} &\mu_{g_n\to\mathbf{x}_n^u}(\mathbf{x}_n^u)\propto \\ &\sum_{\{\theta^u\}_{u=1}^U}\sum_{\{d_n^u\}_{u=1}^U}\prod_{u=1}^{U}\mu_{\theta^u\to g_n}(\theta^u)\prod_{u=1}^{U}\mu_{d_n^u\to g_n}(d_n^u) \\ &\times\int_{\mathbb{C}^{U-1}}p(\mathbf{y}_n|\theta^1,\ldots,\theta^U,\mathbf{x}_n^1,\ldots,\mathbf{x}_n^U,d_n^1,\ldots,d_n^U) \\ &\qquad\times\prod_{u'\neq u}\mu_{\mathbf{x}_n^{u'}\to g_n}(\mathbf{x}_n^{u'})\prod_{u'\neq u}d\mathbf{x}_n^{u'}, \end{aligned} \tag{7}$$

which can be viewed as the likelihood function of $\mathbf{x}_n^u$ for fixed $\mathbf{y}_n$. Messages for the u-th user CFR states in the forward and backward direction are computed recursively using (7)

$$\begin{aligned} \mu_{f_{n+1}^u\to\mathbf{x}_{n+1}^u}(\mathbf{x}_{n+1}^u)&\propto\int p(\mathbf{x}_{n+1}^u|\mathbf{x}_n^u)\mu_{g_n\to\mathbf{x}_n^u}(\mathbf{x}_n^u)\mu_{f_n^u\to\mathbf{x}_n^u}(\mathbf{x}_n^u)d\mathbf{x}_n^u \\ \mu_{f_n^u\to\mathbf{x}_{n-1}^u}(\mathbf{x}_{n-1}^u)&\propto\int p(\mathbf{x}_n^u|\mathbf{x}_{n-1}^u)\mu_{g_n\to\mathbf{x}_n^u}(\mathbf{x}_n^u)\mu_{f_{n+1}^u\to\mathbf{x}_n^u}(\mathbf{x}_n^u)d\mathbf{x}_n^u. \end{aligned} \tag{8}$$

Finally, applying the sum-product rule at the variable node $\mathbf{x}_n^u$, the outcoming messages on the u-th user CFR estimation subgraph are obtained as the product of forward and backward messages in (8)

$$\mu_{\mathbf{x}_n^u\to g_n}(\mathbf{x}_n^u)\propto\mu_{f_n^u\to\mathbf{x}_n^u}(\mathbf{x}_n^u)\mu_{f_{n+1}^u\to\mathbf{x}_n^u}(\mathbf{x}_n^u). \tag{9}$$

B. u-th user demodulation and decoding subgraph

The incoming message on the u-th user demodulation subgraph on to d_n^u is computed from the sum-product rule applied at the factor node g_n as

$$\begin{aligned} &\mu_{g_n\to d_n^u}(d_n^u)\propto \\ &\sum_{\{\theta^u\}_{u=1}^U}\sum_{\{d_n^{u'}\}_{u'\neq u}}\prod_{u=1}^{U}\mu_{\theta^u\to g_n}(\theta^u)\prod_{u'\neq u}\mu_{d_n^{u'}\to g_n}(d_n^{u'}) \\ &\times\int_{\mathbb{C}^U}p(\mathbf{y}_n|\theta^1,\ldots,\theta^U,\mathbf{x}_n^1,\ldots,\mathbf{x}_n^U,d_n^1,\ldots,d_n^U) \\ &\qquad\times\prod_{u=1}^{U}\mu_{\mathbf{x}_n^u\to g_n}(\mathbf{x}_n^u)\prod_{u=1}^{U}d\mathbf{x}_n^u \end{aligned} \tag{10}$$

which can be viewed as the likelihood function of d_n^u for fixed $\mathbf{y}_n$. Finally, regarding the u-th user decoding subgraph, the messages from d_n^u to the bit interleaver π^u and from the bit interleaver π^u to d_n^u, correspond to the bit-level probabilities computed by the standard turbo-demodulation algorithm introduced in [27].

C. u-th user activity detection subgraph

From the sum-product rule, the incoming message from the observation factor node g_n on to the u-th user existence

variable θ^u has the form

$$\begin{aligned}\mu_{g_n\to\theta^u}(\theta^u) \propto \\ \sum_{\{\theta^{u'}\}_{u'\neq u}} \sum_{\{d_n^u\}_{u=1}^U} \prod_{u'\neq u} \mu_{\theta^{u'}\to g_n}(\theta^{u'}) \prod_{u=1}^U \mu_{d_n^u\to g_n}(d_n^u) \\ \times \int_{\mathbb{C}^U} p(\mathbf{y}_n|\theta^1,\ldots,\theta^U,\mathbf{x}_n^1,\ldots,\mathbf{x}_n^U,d_n^1,\ldots,d_n^U) \\ \times \prod_{u=1}^U \mu_{\mathbf{x}_n^u\to g_n}(\mathbf{x}_n^u) \prod_{u=1}^U d\mathbf{x}_n^u\end{aligned} \tag{11}$$

and can be viewed as the likelihood function of θ^u for fixed $\mathbf{y}_n$. In turn, the outcoming message from the u-th user existence variable θ^u on to the observation factor node g_n can be written as

$$\mu_{\theta^u\to g_n}(\theta^u) \propto \prod_{m\neq n} \mu_{g_m\to\theta^u}(\theta^u). \tag{12}$$

Also, the marginal probability mass function (p.m.f) of θ^u

$$P(\theta^u|\mathbf{y}_{1:N}) \propto \prod_{n=0}^{N-1} \mu_{g_n\to\theta^u}(\theta^u) \tag{13}$$

can be used to perform u-th user maximum *a posteriori* activity detection as

$$\hat{\theta^u} = \begin{cases} 1 & \text{if} \quad P(\theta^u=1|\mathbf{y}_{1:N}) > P(\theta^u=0|\mathbf{y}_{1:N}) \\ 0 & \text{otherwise.} \end{cases} \tag{14}$$

D. Message-passing schedule

In our factor graph with cycles, message-passing naturally leads to an iterative algorithm [21]. There is considerable freedom in the selection of the message-passing schedule. Here, we propose a serial schedule, that updates the messages on the subgraphs corresponding to each user in turn instead of simultaneously.

The overall iterative algorithm proceeds as follows. For each iteration, the following steps are executed on each user's subgraph by order of descending transmitted energy. On the u-th user subgraph, depicted in Fig. 3:

1) perform forward-backward CFR estimation for the current user (see Sec. III-A)
2) perform one soft demodulation and soft decoding pass for the current user (see Sec. III-B)
3) update the existence variable probabilities, based on updated CFR marginals and post-decoding symbol-level probabilities for the current user (see Sec. III-C).

E. Message-passing initialization

Initialization is needed at the first iteration to compute (7), (10) and (11). In the absence of CFR estimation at the starting point, messages from CFR states to observation factor nodes $\mu_{\mathbf{x}_n^u\to g_n}(\mathbf{x}_n^u)$, are initialized to the CFR Gaussian priors (2), $\forall(u,n)$. Symbol-level probabilities $\mu_{d_n^u\to g_n}(d_n^u)$ are initialized to a Kronecker delta function if n corresponds to a u-th user pilot subcarrier (since d_n^u is perfectly known) and to the uniform p.m.f if n corresponds to a u-th user data subcarrier (since no prior knowledge on d_n^u is available). For some specific applications, the prior user activity probability can be obtained from traffic models [28]. However, since such prior information is generally unavailable, we assume a worst case scenario where all users are present, that is $\mu_{\theta^u\to g_n}(1)=1$ and $\mu_{\theta^u\to g_n}(0)=0$, $\forall(u,n)$ during the first iteration.

Also, for all iterations, the forward CFR estimation recursion at $n=0$ (resp. the backward CFR estimation recursion at $n=N-1$) in (8) is initialized with the CFR Gaussian prior of each user (2).

F. Complexity issues

Let us consider the u-th user CFR estimation in Sec. III-A. The summation in (7) involves $MU(M+1)^{U-1}$ different integrals for all valid combinations of existing users and their corresponding transmitted symbols. From Sec. III-E, the CFR estimation message computed in the forward (resp. backward) direction in (8) is Gaussian only at the $n=0$ (resp. $n=N-1$), and becomes a Gaussian mixture whose number of mixands grows as the subcarrier index increases (resp. decreases). It follows that each integral in the summation (7) is also a Gaussian mixture whose number of mixands grows with N. Clearly, a similar combinatorial explosion effect occurs for the u-th user demodulation in (10) and the u-th UAD in (11). It follows that, even for moderate values of M, U and N, the complexity of the belief propagation receiver becomes intractable.

IV. Low-complexity message-passing receiver

We seek an alternative to the exact implementation of belief propagation, able to solve the complexity issue raised in Sec. III-F and yet retaining near-optimal performance. To this end, we propose to approximate all continuous-valued messages in Sec. III by Gaussian messages, while preserving the same message-passing schedule and initialization. In this section, we rederive the corresponding messages for per-user CFR estimation in Sec. IV-B, for demodulation and decoding in Sec. IV-C and for UAD in Sec. IV-D, after introducing useful notations in Sec IV-A.

A. Multi-User Interference (MUI) notations

Let us consider the contribution of the u'-th user on the MUI vector affecting all other users on the n-th subcarrier. Its expectation is given by $\hat{\mathbf{H}}_n^{u'}\hat{\mathbf{x}}_{n\backslash n}^{u'}$, where

$$\hat{\mathbf{H}}_n^u = \sum_{\theta^u}\sum_{d_n^u} \mu_{\theta^u\to g_n}(\theta^u)\mu_{d_n^u\to g_n}(d_n^u)\theta^u\mathbf{H}_n^u(d_n^u), \forall u \tag{15}$$

and its covariance

$$\begin{aligned}\mathbf{I}_n^{u'} = \sum_{\theta^{u'}}\sum_{d_n^{u'}} \mu_{\theta^{u'}\to g_n}(\theta^{u'})\mu_{d_n^{u'}\to g_n}(d_n^{u'})\times \\ \Big\{\theta^{u'}\mathbf{H}_n^{u'}(d_n^{u'})\mathbf{P}_{n\backslash n}^{u'}\mathbf{H}_n^{u'}(d_n^{u'})^H + \\ (\theta^{u'}\mathbf{H}_n^{u'}(d_n^{u'}) - \hat{\mathbf{H}}_n^{u'})\hat{\mathbf{x}}_{n\backslash n}^{u'}\hat{\mathbf{x}}_{n\backslash n}^{u'}{}^H(\theta^{u'}\mathbf{H}_n^{u'}(d_n^{u'}) - \hat{\mathbf{H}}_n^{u'})^H\Big\},\end{aligned} \tag{16}$$

accounts for both the residual CFR, data and existence uncertainty on the u'-th user MUI contribution.

B. u-th user CFR estimation subgraph

As per hypothesis, the message from the CFR state of user $u' \neq u$ on to the factor node g_n is approximated as the Gaussian p.d.f.

$$\mu_{\mathbf{x}_n^{u'} \to g_n}(\mathbf{x}_n^{u'}) \propto \mathcal{N}_C(\mathbf{x}_n^{u'} : \hat{\mathbf{x}}_{n\backslash n}^{u'}, \mathbf{P}_{n\backslash n}^{u'}), \tag{17}$$

whose mean and covariance will be derived later in (23).

From (5), we get the likelihood of all unknowns for fixed $\mathbf{y}_n$

$$p(\mathbf{y}_n|\theta^1, \ldots, \theta^U, \mathbf{x}_n^1, \ldots, \mathbf{x}_n^U, d_n^1, \ldots, d_n^U) = \mathcal{N}_C\left(\mathbf{y}_n : \sum_{u=1}^{U} \theta^u \mathbf{H}_n^u(d_n^u)\mathbf{x}_n^u, \mathbf{R}\right). \tag{18}$$

Injecting (17) and (18) into (7), the likelihood function of $\mathbf{x}_n^u$ for fixed $\mathbf{y}_n$ becomes (see [29, p. 40])

$$\begin{aligned}\mu_{g_n \to \mathbf{x}_n^u}(\mathbf{x}_n^u) \propto & \sum_{\{\theta^u\}_{u=1}^U} \sum_{\{d_n^u\}_{u=1}^U} \prod_{u=1}^{U} \mu_{\theta^u \to g_n}(\theta^u) \prod_{u=1}^{U} \mu_{d_n^u \to g_n}(d_n^u) \\ & \times \mathcal{N}_C\Big(\mathbf{y}_n : \theta^u \mathbf{H}_n^u(d_n^u)\mathbf{x}_n^u + \sum_{u' \neq u} \theta^{u'} \mathbf{H}_n^{u'}(d_n^{u'})\hat{\mathbf{x}}_{n\backslash n}^{u'}, \\ & \sum_{u' \neq u} \theta^{u'} \mathbf{H}_n^{u'}(d_n^{u'})\mathbf{P}_{n\backslash n}^{u'} \mathbf{H}_n^{u'}(d_n^{u'})^H + \mathbf{R}\Big).\end{aligned} \tag{19}$$

Now, collapsing (19) to a single Gaussian, we obtain

$$\mu_{g_n \to \mathbf{x}_n^u}(\mathbf{x}_n^u) \propto \mathcal{N}_C\left(\mathbf{y}_n : \hat{\mathbf{H}}_n^u \mathbf{x}_n^u + \sum_{u' \neq u} \hat{\mathbf{H}}_n^{u'} \hat{\mathbf{x}}_{n\backslash n}^{u'}, \hat{\mathbf{D}}_n^u + \sum_{u' \neq u} \mathbf{I}_n^{u'} + \mathbf{R}\right), \tag{20}$$

where the u-th user's desired signal contribution on the n-th subcarrier for the sake of CFR estimation has expectation $\hat{\mathbf{H}}_n^u \mathbf{x}_n^u$ and covariance

$$\begin{aligned}\hat{\mathbf{D}}_n^u = & \sum_{\theta^u} \sum_{d_n^u} \mu_{\theta^u \to g_n}(\theta^u) \mu_{d_n^u \to g_n}(d_n^u) \\ & \times (\theta^u \mathbf{H}_n^u(d_n^u) - \hat{\mathbf{H}}_n^u)(\theta^u \mathbf{H}_n^u(d_n^u) - \hat{\mathbf{H}}_n^u)^H.\end{aligned} \tag{21}$$

The proof of (20) is postponed to Appendix A.

Injecting (20) into (8), forward-backward CFR estimation messages have the form

$$\begin{aligned}&\mu_{f_n^u \to \mathbf{x}_n^u}(\mathbf{x}_n^u) \propto \mathcal{N}_C(\mathbf{x}_n^u : \hat{\mathbf{x}}_{n|n-1}^u, \mathbf{P}_{n|n-1}^u) \\ &\mu_{f_{n+1}^u \to \mathbf{x}_n^u}(\mathbf{x}_n^u) \propto \mathcal{N}_C(\mathbf{x}_n^u : \hat{\mathbf{x}}_{n|n+1:N-1}^u, \mathbf{P}_{n|n+1:N-1}^u),\end{aligned} \tag{22}$$

whose mean and covariance are updated with the standard Kalman filter [30]. Finally, injecting (22) into (9), the outcoming message from the u-th CFR estimation subgraph, takes the extrinsic two-filter Kalman smoother form [30]

$$\mu_{\mathbf{x}_n^u \to g_n}(\mathbf{x}_n^u) \propto \mathcal{N}_C(\mathbf{x}_n^u : \hat{\mathbf{x}}_{n\backslash n}^u, \mathbf{P}_{n\backslash n}^u), \tag{23}$$

whose mean and covariance are computed as

$$\begin{cases}\mathbf{P}_{n\backslash n}^u = \mathbf{P}_{n|n-1}^u \left[\mathbf{P}_{n|n-1}^u + \mathbf{P}_{n|n+1:N-1}^u\right]^{-1} \mathbf{P}_{n|n+1:N-1}^u \\ \hat{\mathbf{x}}_{n\backslash n}^u = \mathbf{P}_{n\backslash n}^u \left[{\mathbf{P}_{n|n-1}^u}^{-1} \hat{\mathbf{x}}_{n|n-1}^u + {\mathbf{P}_{n|n+1:N-1}^u}^{-1} \hat{\mathbf{x}}_{n|n+1:N-1}^u\right].\end{cases}$$

C. u-th user demodulation and decoding subgraph

Using the same method as in Sec. IV-B, we now lower the complexity of soft demodulation. Namely, we rewrite (10) using (17) and (18) as (see [29, p. 40])

$$\begin{aligned}\mu_{g_n \to d_n^u}(d_n^u) \propto & \sum_{\{\theta^u\}_{u=1}^U} \sum_{\{d_n^{u'}\}_{u' \neq u}} \prod_{u=1}^{U} \mu_{\theta^u \to g_n}(\theta^u) \prod_{u' \neq u} \mu_{d_n^{u'} \to g_n}(d_n^{u'}) \\ & \times \mathcal{N}_C\Big(\mathbf{y}_n : \theta^u \mathbf{H}_n^u(d_n^u)\hat{\mathbf{x}}_{n\backslash n}^u + \sum_{u' \neq u} \theta^{u'} \mathbf{H}_n^{u'}(d_n^{u'})\hat{\mathbf{x}}_{n\backslash n}^{u'}, \\ & \theta^u \mathbf{H}_n^u(d_n^u)\mathbf{P}_{n\backslash n}^u \mathbf{H}_n^u(d_n^u)^H + \\ & \sum_{u' \neq u} \theta^{u'} \mathbf{H}_n^{u'}(d_n^{u'})\mathbf{P}_{n\backslash n}^{u'} \mathbf{H}_n^{u'}(d_n^{u'})^H + \mathbf{R}\Big).\end{aligned} \tag{24}$$

Collapsing (24) to a single Gaussian, the likelihood of d_n^u for fixed $\mathbf{y}_n$ simplifies to

$$\begin{aligned}\mu_{g_n \to d_n^u}(d_n^u) \propto & \\ \mathcal{N}_C\Big(\mathbf{y}_n : \tilde{\mathbf{H}}_n^u \hat{\mathbf{x}}_{n\backslash n}^u + \sum_{u' \neq u} \hat{\mathbf{H}}_n^{u'} \hat{\mathbf{x}}_{n\backslash n}^{u'}, \tilde{\mathbf{D}}_n^u + \sum_{u' \neq u} \mathbf{I}_n^{u'} + \mathbf{R}\Big),\end{aligned} \tag{25}$$

where the u-th user's desired signal contribution on the n-th subcarrier for the sake of demodulation has expectation $\tilde{\mathbf{H}}_n^u \hat{\mathbf{x}}_{n\backslash n}^u$, where

$$\tilde{\mathbf{H}}_n^u = \sum_{\theta^u} \mu_{\theta^u \to g_n}(\theta^u) \theta^u \mathbf{H}_n^u(d_n^u), \tag{26}$$

and covariance

$$\begin{aligned}\tilde{\mathbf{D}}_n^u = & \sum_{\theta^u} \mu_{\theta^u \to g_n}(\theta^u) \times \\ & \Big\{\theta^u \mathbf{H}_n^u(d_n^u)\mathbf{P}_{n\backslash n}^u \mathbf{H}_n^u(d_n^u)^H \\ & + (\theta^u \mathbf{H}_n^u(d_n^u) - \tilde{\mathbf{H}}_n^u)\hat{\mathbf{x}}_{n\backslash n}^u {\hat{\mathbf{x}}_{n\backslash n}^u}^H (\theta^u \mathbf{H}_n^u(d_n^u) - \tilde{\mathbf{H}}_n^u)^H\Big\}.\end{aligned} \tag{27}$$

The proof of (25) is omitted since it is similar to Appendix A.

Note that message-passing on the decoding subgraph remains unchanged from the description in Sec. III-B.

D. u-th user activity detection subgraph

Again, using the same method as in Sec. IV-B, we now lower the complexity of u-th user soft activity detection. Namely, we rewrite (11) using (17) and (18) as (see [29, p. 40])

$$\begin{aligned}\mu_{g_n \to \theta^u}(\theta^u) \propto & \sum_{\{\theta^{u'}\}_{u' \neq u}} \sum_{\{d_n^u\}_{u=1}^U} \prod_{u' \neq u} \mu_{\theta^{u'} \to g_n}(\theta^{u'}) \prod_{u=1}^{U} \mu_{d_n^u \to g_n}(d_n^u) \\ & \times \mathcal{N}_C\Big(\mathbf{y}_n : \theta^u \mathbf{H}_n^u(d_n^u)\hat{\mathbf{x}}_{n\backslash n}^u + \sum_{u' \neq u} \theta^{u'} \mathbf{H}_n^{u'}(d_n^{u'})\hat{\mathbf{x}}_{n\backslash n}^{u'}, \\ & \theta^u \mathbf{H}_n^u(d_n^u)\mathbf{P}_{n\backslash n}^u \mathbf{H}_n^u(d_n^u)^H + \\ & \sum_{u' \neq u} \theta^{u'} \mathbf{H}_n^{u'}(d_n^{u'})\mathbf{P}_{n\backslash n}^{u'} \mathbf{H}_n^{u'}(d_n^{u'})^H + \mathbf{R}\Big).\end{aligned} \tag{28}$$

Collapsing (28) to a single Gaussian, the likelihood of θ^u for fixed $\mathbf{y}_n$ simplifies to

$$\mu_{g_n\to\theta^u}(\theta^u) \propto \mathcal{N}_C\Big(\mathbf{y}_n : \bar{\mathbf{H}}_n^u\hat{\mathbf{x}}_{n\backslash n}^u + \sum_{u'\neq u}\hat{\mathbf{H}}_n^{u'}\hat{\mathbf{x}}_{n\backslash n}^{u'}, \bar{\mathbf{D}}_n^u + \sum_{u'\neq u}\mathbf{I}_n^{u'} + \mathbf{R}\Big), \tag{29}$$

where the u-th user's desired signal contribution on the n-th subcarrier for the sake of UAD has expectation $\bar{\mathbf{H}}_n^u\hat{\mathbf{x}}_{n\backslash n}^u$, where

$$\bar{\mathbf{H}}_n^u = \sum_{d_n^u}\mu_{d_n^u\to g_n}(d_n^u)\theta^u\mathbf{H}_n^u(d_n^u), \tag{30}$$

and covariance

$$\bar{\mathbf{D}}_n^u = \sum_{d_n^u}\mu_{d_n^u\to g_n}(d_n^u)\times \Big\{\theta^u\mathbf{H}_n^u(d_n^u)\mathbf{P}_{n\backslash n}^u\mathbf{H}_n^u(d_n^u)^H + (\theta^u\mathbf{H}_n^u(d_n^u) - \bar{\mathbf{H}}_n^u)\hat{\mathbf{x}}_{n\backslash n}^u{\hat{\mathbf{x}}_{n\backslash n}^u}^H(\theta^u\mathbf{H}_n^u(d_n^u) - \bar{\mathbf{H}}_n^u)^H\Big\}. \tag{31}$$

The proof of (29) is omitted since it is similar to Appendix A.

Note that the computation of (12)-(14) remains unchanged.

E. Complexity evaluation

Let N_{it} denote the number of message-passing iterations. The computational compexity per-user and per-subcarrier of

- each MUI term's expectation and covariance calculation in Sec. IV-A is $\mathcal{O}(MN_RN_{it})$ and $\mathcal{O}(MN_R^2N_{it})$, respectively
- CFR estimation in Sec. IV-B is $\mathcal{O}(N_R^3N_{it})$, due to matrix inversion in Kalman filtering
- soft demodulation in Sec. IV-C is $\mathcal{O}(MN_R^3N_{it})$, due to matrix inversion in (25) for each symbol in the M-ary alphabet
- soft UAD in Sec. IV-D is $\mathcal{O}(2N_R^3N_{it})$, due to matrix inversion in (29) for each existence variable in $\{0,1\}$.

Consequently, we obtain the desirable property that the computational complexity of the low-complexity message-passing receiver grows only linearly with U, the maximum number of users, thus effectively solving the combinatorial explosion issue related to the belief propagation receiver of Sec. III.

V. Numerical results

In this section, we present numerical results that compare several receivers:

- benchmark receivers with separate UAD and CEMUDD
- the joint UAD-CEMUDD receiver proposed in Sec. IV
- the proposed receiver in Sec. IV, based on perfect channel state information (CSI)
- the proposed receiver in Sec. IV, based on perfect UAD.

The comparison is performed in terms of bit error rate (BER), CFR mean square error (MSE), probability of false alarm (P_{fa}) and probability of missed detection (P_{md}) for each user. Note that the computation of the BER and CFR MSE for the u-th user takes into account only those OFDM blocks for which user activity is detected (i.e. $\hat{\theta}^u = 1$ in (14)).

A. Setup

We consider the uplink of a multi-user system with a maximum of U equal-energy users equipped with one transmit antenna. For each active user, the transmission is based on a rate-$1/2$ recursive systematic convolutional encoder, with generator polynomials $(1, 5/7)$ in octal, followed by user-specific random interleaving. For bit to symbol mapping, quadrature phase shift keying (QPSK) or $8/16$-ary quadrature amplitude modulation ($8/16$-QAM) is used, followed by OFDM modulation with $N = 1024$ subcarriers. All CIRs in Sec. II-B are simulated independently for each OFDM block according to a Rayleigh fading model with an exponentially decreasing power delay profile that has a decay constant of three taps. A CP of size $N/8 = 128$ samples is inserted, so that asynchronous access with large timing misalignments between users can be tolerated. At the destination node, the assumed model for each user's CFR is the Gauss-Markov model (3). The driving noise parameter ζ, introduced to compensate for the modeling mismatch, has been optimized via numerical simulations to 10. Also, in order to avoid underdetermined reception, we assume that the cardinality of the active user set is less than or equal to the number of receive antennas, N_R.

B. Cognitive radio scenario

We address the problem of dynamically leasing an under-utilized frequency band to a secondary (unlicensed) user (SU) without causing harmful interference to the primary (licensed) user (PU) [1]. This scenario corresponds to $U = 1$, where the single user (user 1) plays the role of the PU and the destination plays the role of the SU. Since the transmission of user 1 may occur or cease at any time, in the absence of prior information we model the existence variable θ^1 as a binary random variable, that is independently distributed for each OFDM block according to a Bernoulli distribution with $P(\theta^1 = 0) = P(\theta^1 = 1) = 0.5$. Here, we use QPSK modulation and $N_R = 1$, which is sufficient to ensure identifiability. Additionally, we chose a benchmark method that applies the two following steps on each OFDM block:

- UAD: conventional CFAR energy detection [4], where P_{fa} is fixed to 10^{-5}
- CEMUDD: the proposed method in Sec. IV where θ^1 is fixed to the value returned by the energy detector.

1) Convergence analysis: A convenient semi-analytical tool to assess the convergence properties of iterative receivers is the EXIT chart [31]. In Sec. V-B2, we will show that the proposed joint UAD-CEMUDD incurs no BER nor CFR MSE performance loss wrt the perfect UAD case. Therefore, we restrict our analysis to the proposed receiver under perfect UAD. The behavior of an iterative receiver is predicted by plotting the EXIT functions of its constituent components. Let I_A^{dec} (resp. I_E^{dec}) denote the mutual information (MI) between the encoded bits and the *a priori* LLRs at the decoder input (resp. the MI between the encoded bits and the *extrinsic* LLRs at the decoder output), the decoder EXIT function has the form

$$I_E^{dec} = T^{dec}(I_A^{dec})$$

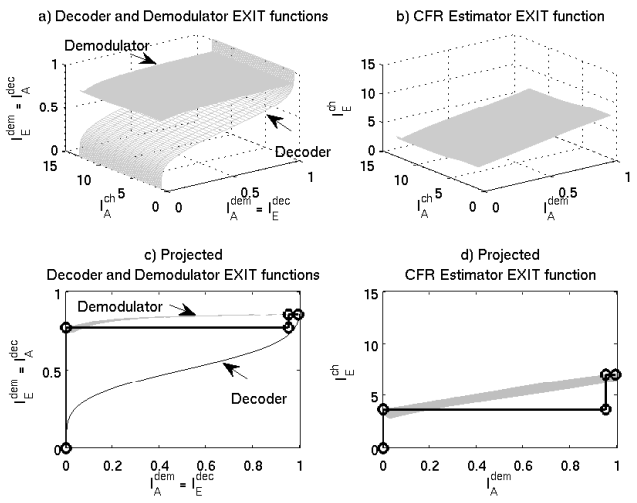

Fig. 4. Proposed method with perfect UAD in the cognitive radio scenario using QPSK with $E_s^1/N_0 = 10$ dB - a) and b): 3D-EXIT functions - c) and d): Projected EXIT functions along with the simulated EXIT trajectory (circles).

and is obtained via the standard Monte Carlo simulation method decribed in [31]. Similarly, we let I_A^{dem} (resp. I_E^{dem}) denote the MI between the encoded bits and the *a priori* LLRs at the soft demodulator input (resp. the MI between the encoded bits and the *extrinsic* LLRs at the soft demodulator output). Additionally, we define I_A^{ch} (resp. I_E^{ch}) as the MI between the true and the estimated complex CFR coefficients at the receive antennas before CFR re-estimation (resp. the MI between the true and the estimated complex CFR coefficients at the receive antennas after CFR re-estimation) [32]. The CFR estimator and demodulator EXIT functions have the form

$$\begin{aligned} I_E^{ch} &= T^{ch}(I_A^{ch}, I_A^{dem}, E_s^1/N_0) \\ I_E^{dem} &= T^{dem}(I_A^{ch}, I_A^{dem}, E_s^1/N_0), \end{aligned} \tag{32}$$

where E_s^1/N_0 denotes the per-symbol signal-to-noise ratio (SNR) measure. The EXIT functions in (32) are obtained via the Monte Carlo simulation method decribed in [32]. Note that these EXIT functions could easily be generalized for a maximum number of users $U > 1$, but at the expense of increased dimensionality.

Fig. 4 a) (resp. 4 b)) illustrates the decoder and demodulator EXIT functions (resp. CFR estimator EXIT function) at $E_s^1/N_0 = 10$ dB. We also plot simulated EXIT trajectories in Fig. 4 c) and 4 d), obtained by collecting CFR estimates and extrinsic LLRs at the demodulator/decoder output for several iterations of the proposed receiver during 5000 consecutive codewords. For the sake of readability, simulated EXIT trajectories are compared with EXIT functions projected on 2D planes [33]. As expected, EXIT trajectories obtained via Monte Carlo simulations follow a zig-zag pattern delimited by the EXIT functions. It can be seen that convergence is reached after two iterations for this scenario.

2) BER and CFR MSE performance: Fig. 5 presents the BER performances of the aforementioned receivers for QPSK modulation. Convergence is reached within two iterations

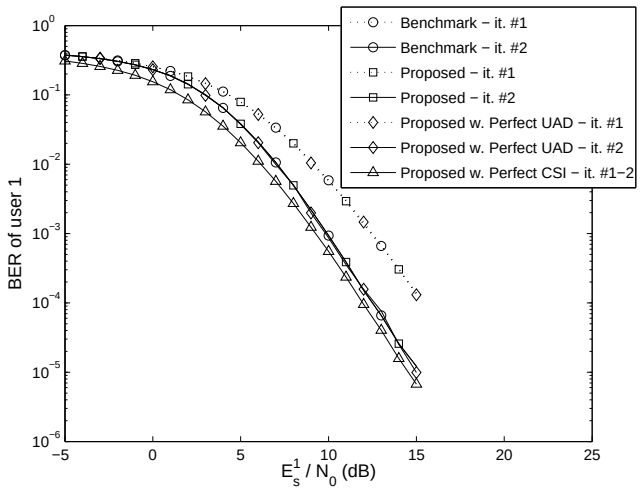

Fig. 5. BER of iterative receivers for the cognitive radio scenario: QPSK modulation, 2 iterations.

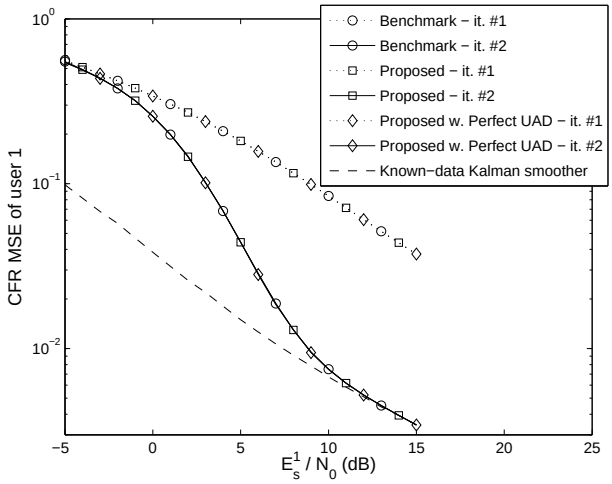

Fig. 6. CFR MSE of iterative receivers for the cognitive radio scenario: QPSK modulation, 2 iterations.

for all receivers. We observe that no BER performance loss is incurred for the proposed joint UAD-CEMUDD wrt the perfect UAD case. Also, the power efficiency loss wrt the perfect CSI case is only 0.5 dB. It can be concluded that the Gaussian approximation introduced for the sake of obtaining fixed-complexity message update rules in the CFR estimation and UAD stages has only a limited impact on the overall performance.

Moreover, the benchmark method and the proposed joint UAD-CEMUDD differ only in the way UAD is performed. As a result, there is no noticeable difference in terms of BER. Similar conclusions can be drawn for the CFR MSE performances, shown in Fig. 6. Interestingly, the proposed low-complexity receiver exhibits no performance loss compared to the lower bound given by the genie-aided Kalman smoother at high SNR.

3) False alarm and missed detection performance: Fig. 7 shows the false alarm and missed detection probabilities for all

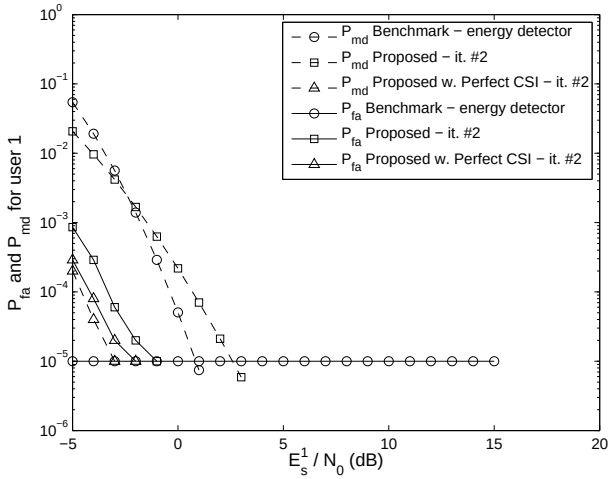

Fig. 7. P_{fa} and P_{md} of iterative receivers for the cognitive radio scenario: QPSK modulation, 2 iterations.

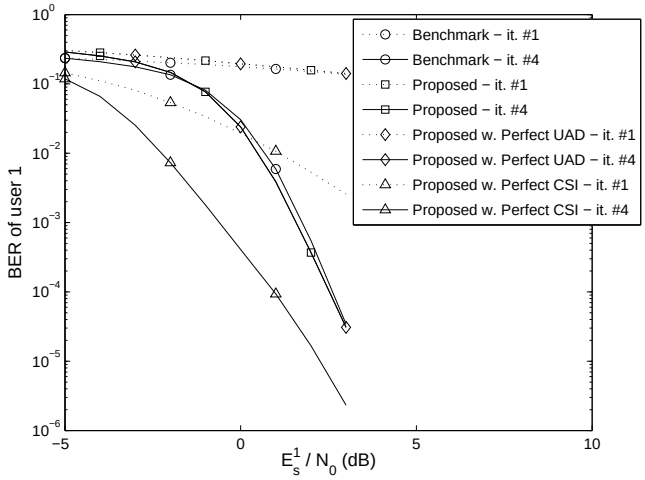

Fig. 8. BER of iterative receivers for the maximum user activity scenario: QPSK modulation, 4 iterations, user 1.

considered receivers. Note that in terms of P_{md} (resp. P_{fa}), the proposed joint UAD-CEMUDD is 5 dB (resp. 1 dB) away from the perfect CSI case. This result can be interpreted as follows: in the presence of user 1, poor SNRs yield unreliable soft symbols and CFR estimates (see Fig. 5-6) and therefore prevent the user activity probabilities (29) to discriminate the useful signal from the background noise.

Now, comparing the proposed joint UAD-CEMUDD with the benchmark energy detector, we obtain the intuitively satisfying result that a higher P_{fa} yields a lower P_{md} and vice versa. The obvious advantage of joint UAD-CEMUDD over the energy detector is that the P_{fa} need not be preset to a target value, but adjusts itself optimally based on existing SNR conditions. Furthermore, energy thresholding performs hard UAD, while reliability information on the UAD is available for joint UAD-CEMUDD, based on (13). Such information is valuable to the destination, which can choose not to trigger SU transmission in case of unreliable PU activity detection.

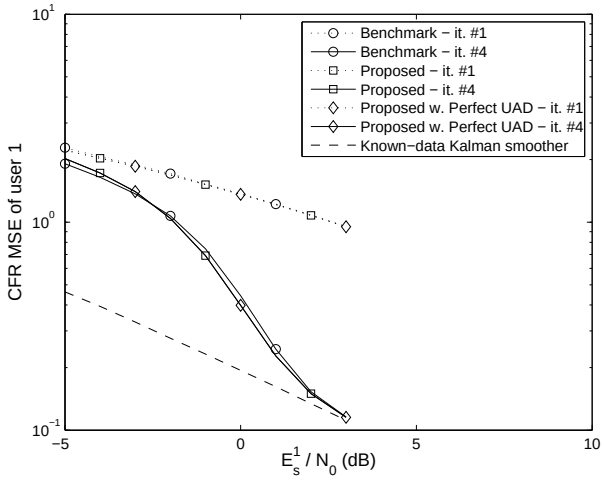

Fig. 9. CFR MSE of iterative receivers for the maximum user activity scenario: QPSK modulation, 4 iterations, user 1.

C. Maximum user activity scenario - QPSK modulation

We now focus on a test case where the sparse user activity assumption in [17]-[18] is violated. We consider a dynamic scenario, where the U users are either all active (fully-loaded situation) or all inactive (idle spectrum situation enabling SU transmission). Here, we choose QPSK modulation, $U = 4$ and $N_R = 4$, which is sufficient to ensure identifiability.

We choose as a benchmark method a modified version of the proposed receiver with perfect UAD, where exact user activity knowledge is replaced by the following hard UAD estimate for each user. Borrowing the user validation statistic from protocol-based methods [7]-[8], we define the correlation with normalized power by correlating the frequency-domain observations with the reconstructed u-th user's signal at the numerator

$$R^u = \frac{|\sum_{n=0}^{N-1}(\mathbf{H}_n^u(\hat{d}_n^u)\hat{\mathbf{x}}_{n\backslash n}^u)^H\mathbf{y}_n|}{\sqrt{\sum_{n=0}^{N-1}\mathbf{y}_n^H\mathbf{y}_n}} \tag{33}$$

where $\hat{d}_n^u$ is the post-decoding u-th user detected symbol on the n-th subcarrier. We seek an hypothesis test of the form

$$\hat{\theta^u} = \begin{cases} 1 & \text{if} \quad R^u > \lambda_t \\ 0 & \text{otherwise} \end{cases} \tag{34}$$

where λ_t is a pre-defined threshold such that $P_{fa} \lesssim 10^{-5}$. Since an analytical model for the decision statistic p.d.f. is unavailable, histograms obtained via Monte Carlo simulations were used to determine a value of λ_t suitable $\forall(U, N_R)$ as $13.0508 * \sigma^u/2.0$, where

$$\sigma^u = \sqrt{\frac{\sum_{n=0}^{N-1}\text{trace}\,(\mathbf{P}_{n\backslash n}^u)}{N \times N_R}} \tag{35}$$

denotes the u-th user's standard deviation of the channel estimation error per receive antenna.

Due to lack of space, upcoming numerical results are presented only for the user with the worst BER, i.e. user 1.

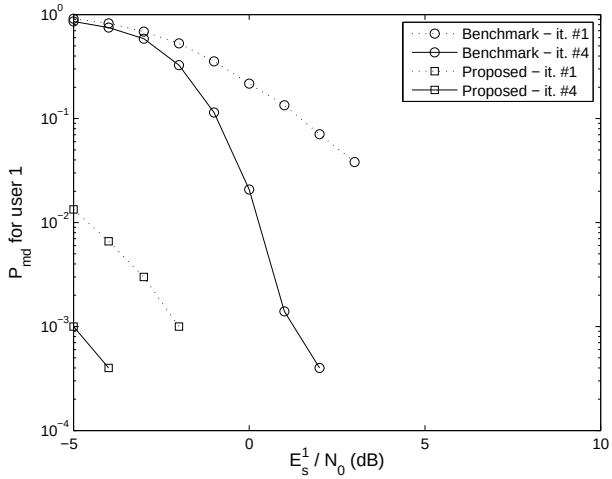

Fig. 10. P_{md} of iterative receivers for the maximum user activity scenario: QPSK modulation, 4 iterations, user 1.

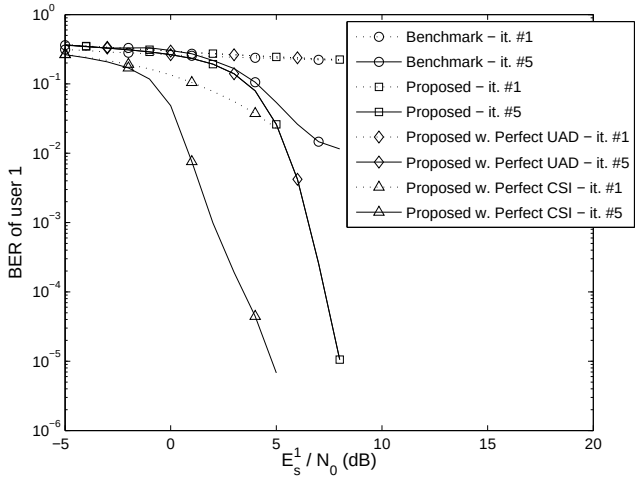

Fig. 11. BER of iterative receivers for the maximum user activity scenario: 8-QAM modulation, 5 iterations, user 1.

Although not shown, the performances for all other users are only slightly better.

1) BER and CFR MSE performance: Fig. 8 depicts the BER performances of the aforementioned receivers for QPSK modulation. Convergence is reached within four iterations for all receivers. In contrats to Fig. 5, we notice the higher slope of the BER versus SNR curve, which shows the ability of the proposed method to take advantage of receive antenna diversity when $N_R > 1$. As can be seen, no BER performance loss is incurred for the proposed joint UAD-CEMUDD wrt the perfect UAD case. Consequently, the proposed scheme leads to near optimal UAD. Also, the BER of the proposed scheme is only 1 dB away from the perfect CSI case at BER of 2×10^{-5}. Moreover, the BER of the benchmark method is only slightly worse than its proposed joint UAD-CEMUDD counterpart, since both methods differ only in the way UAD is performed. This behavior is also confirmed by the CFR MSE performances, shown in Fig. 9.

2) False alarm and missed detection performance: The measured false alarm probability is below 10^{-4} for all receivers over the entire SNR range under consideration. Fig. 10 compares the missed detection probability of the proposed joint UAD-CEMUDD and the benchmark method. When convergence is reached, that is at iteration 4, a 6 dB SNR increase is needed by the benchmark to reach the same P_{md} as the proposed algorithm. Remarkably, the proposed algorithm has outstanding UAD performances even at negative SNRs.

D. Maximum user activity scenario - higher order modulation

We now consider exactly the same setting as in Sec. V-C, but replacing QPSK by a higher order modulation, that is $8/16$-QAM. In particular, the same benchmark as in Sec. V-C is considered. Again, only the worst-user performance is shown and convergence is reached within five iterations for all receivers.

1) BER and CFR MSE performance: Fig. 11 (resp. Fig. 14) presents the BER performances for 8-QAM (resp. 16-QAM) modulation. Again, no BER performance loss is incurred for the proposed joint UAD-CEMUDD wrt the perfect UAD case, which confirms the quasi-optimality of the proposed scheme in terms of UAD. Also, the proposed method has only a 3 dB (resp. 5 dB) SNR loss over the perfect CSI case at a BER level of 10^{-5}. However, this time the BER of the benchmark method is much worse than its proposed joint UAD-CEMUDD counterpart. Indeed, the BER of the benchmark converges to an error floor, which can be attributed to erroneous UAD. CFR MSE results presented in Fig. 12 (resp. Fig. 15) confirm this explanation, as the proposed receiver is far superior to the benchmark scheme for 8-QAM (resp. 16-QAM) modulation.

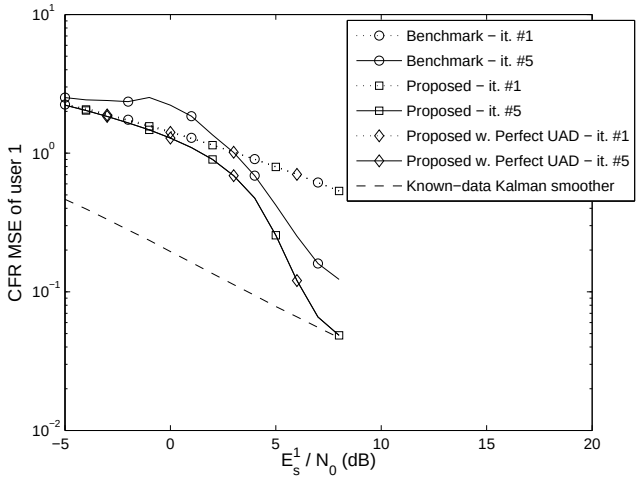

Fig. 12. CFR MSE of iterative receivers for the maximum user activity scenario: 8-QAM modulation, 5 iterations, user 1.

2) False alarm and missed detection performance: The measured false alarm probability is below 10^{-4} for all receivers over the entire SNR range under consideration. Fig. 13 (resp. Fig. 16) compares the missed detection probability of the proposed joint UAD-CEMUDD and the benchmark method for 8-QAM (resp. 16-QAM) modulation. It is seen that the

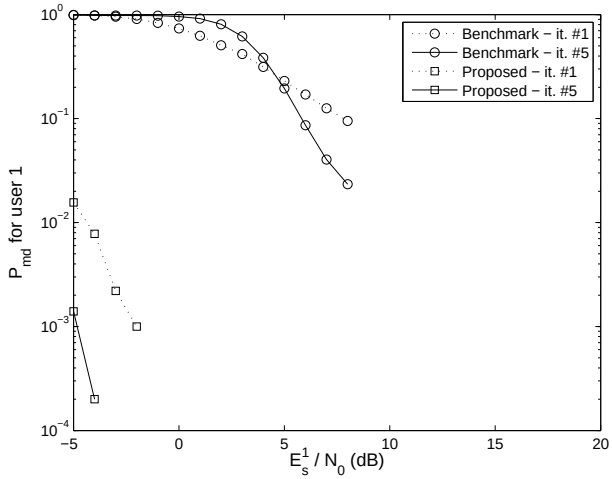

Fig. 13. P_{md} of iterative receivers for the maximum user activity scenario: 8-QAM modulation, 5 iterations, user 1.

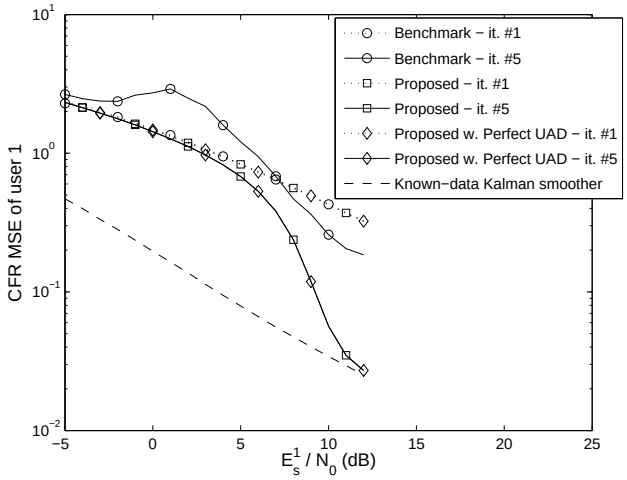

Fig. 15. CFR MSE of iterative receivers for the maximum user activity scenario: 16-QAM modulation, 5 iterations, user 1.

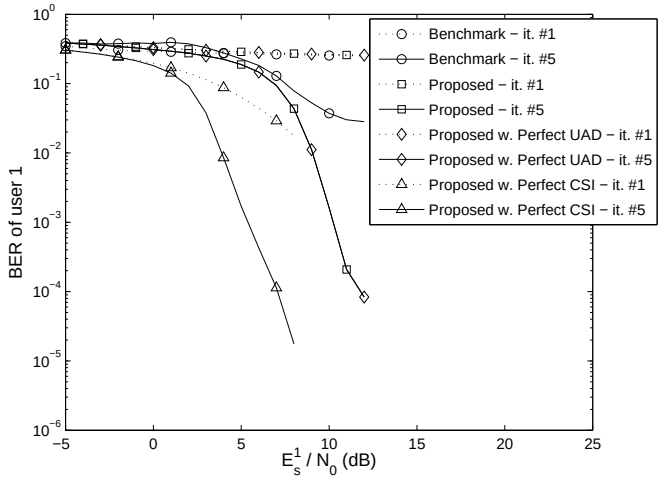

Fig. 14. BER of iterative receivers for the maximum user activity scenario: 16-QAM modulation, 5 iterations, user 1.

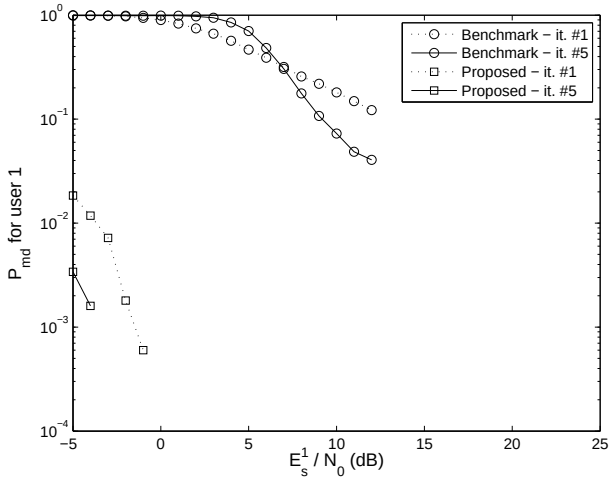

Fig. 16. P_{md} of iterative receivers for the maximum user activity scenario: 16-QAM modulation, 5 iterations, user 1.

benchmark has a high P_{md} wrt the proposed algorithm at medium to high SNR. Comparing with the benchmark method, one may conclude that the proposed algorithm is a much better alternative in terms of UAD for $8/16$-QAM.

VI. Conclusion

In this paper, a generalization of multi-user detection to the case of an unknown and highly dynamic number of users was introduced in the context of multi-antenna OFDM receivers. The proposed method performs joint user activity detection, channel estimation, symbol detection and decoding based on a graphical model approach. A distinctive feature of the resulting message-passing receiver is its linear complexity increase with the maximum number of users. This result is achieved by introducing a suitable Gaussian approximation, allowing successive detection and estimation for all users. Numerical results confirmed the ability of the proposed method to provide robust active user set recovery compared to conventional schemes, while maintaining a high antenna diversity order in dynamic channels. Due to the flexibility of the proposed BICM-based scheme, the present work is easily adaptable to higher order modulations and state-of-the art codes such as LDPC, turbo or polar codes.

Future extensions of this work will consider the design of similar systems with more elaborate non-orthogonal multiple access (NOMA) waveforms [18], [34], as well as users equipped with more than one antenna at the transmitter side. In addition, the potential of performance optimization based on non-uniform transmit energy allocation [34] will also be investigated.

APPENDIX A

We assume proper normalization of user activity and symbol p.m.f.s, $\forall(u,n)$

$$\begin{aligned}\sum_{\theta^u}\mu_{\theta^u\to g_n}(\theta^u)&=1\\ \sum_{d_n^u}\mu_{d_n^u\to g_n}(d_n^u)&=1.\end{aligned}\tag{36}$$

We wish to collapse the Gaussian mixture (19) to a single Gaussian of the form $\mathcal{N}_C(\mathbf{y}_n:\mathbf{m}_n(\mathbf{x}_n^u),\mathbf{S}_n(\mathbf{x}_n^u))$. Applying moment-matching, we obtain the expectation of (19) as [29, p. 106]

$$\begin{aligned}&\mathbf{m}_n(\mathbf{x}_n^u)\\ &=\sum_{\{\theta^u\}_{u=1}^U}\sum_{\{d_n^u\}_{u=1}^U}\prod_{u=1}^U\mu_{\theta^u\to g_n}(\theta^u)\prod_{u=1}^U\mu_{d_n^u\to g_n}(d_n^u)\\ &\quad\times\left[\theta^u\mathbf{H}_n^u(d_n^u)\mathbf{x}_n^u+\sum_{u'\neq u}\theta^{u'}\mathbf{H}_n^{u'}(d_n^{u'})\hat{\mathbf{x}}_{n\backslash n}^{u'}\right].\end{aligned}$$

Using the distributivity of multiplication over addition

$$\begin{aligned}&\mathbf{m}_n(\mathbf{x}_n^u)=\\ &\left(\sum_{\theta^u}\sum_{d_n^u}\mu_{\theta^u\to g_n}(\theta^u)\mu_{d_n^u\to g_n}(d_n^u)\theta^u\mathbf{H}_n^u(d_n^u)\mathbf{x}_n^u\right)\\ &\times\left(\sum_{\{\theta^{u'}\}_{u'\neq u}}\sum_{\{d_n^{u'}\}_{u'\neq u}}\prod_{u'\neq u}\mu_{\theta^{u'}\to g_n}(\theta^{u'})\prod_{u'\neq u}\mu_{d_n^{u'}\to g_n}(d_n^{u'})\right)\\ &+\left(\sum_{\{\theta^{u'}\}_{u'\neq u}}\sum_{\{d_n^{u'}\}_{u'\neq u}}\prod_{u'\neq u}\mu_{\theta^{u'}\to g_n}(\theta^{u'})\prod_{u'\neq u}\mu_{d_n^{u'}\to g_n}(d_n^{u'})\right.\\ &\qquad\left.\times\sum_{u'\neq u}\theta^{u'}\mathbf{H}_n^{u'}(d_n^{u'})\hat{\mathbf{x}}_{n\backslash n}^{u'}\right)\\ &\times\left(\sum_{\theta^u}\sum_{d_n^u}\mu_{\theta^u\to g_n}(\theta^u)\mu_{d_n^u\to g_n}(d_n^u)\right)\end{aligned}$$

which, using (36), simplifies to

$$\begin{aligned}\mathbf{m}_n(\mathbf{x}_n^u)&=\hat{\mathbf{H}}_n^u\mathbf{x}_n^u\\ &+\sum_{\{\theta^{u'}\}_{u'\neq u}}\sum_{\{d_n^{u'}\}_{u'\neq u}}\prod_{u'\neq u}\mu_{\theta^{u'}\to g_n}(\theta^{u'})\prod_{u'\neq u}\mu_{d_n^{u'}\to g_n}(d_n^{u'})\\ &\qquad\times\sum_{u'\neq u}\theta^{u'}\mathbf{H}_n^{u'}(d_n^{u'})\hat{\mathbf{x}}_{n\backslash n}^{u'}.\end{aligned}$$

The first (resp. second) term in the previous equation is the expected signal contribution of (resp. the expected MUI affecting) the u-th user on the n-th subcarrier. Now, exchanging the order of summations in the second term and exploiting (36) leads to

$$\mathbf{m}_n(\mathbf{x}_n^u)=\hat{\mathbf{H}}_n^u\mathbf{x}_n^u+\sum_{u'\neq u}\hat{\mathbf{H}}_n^{u'}\hat{\mathbf{x}}_{n\backslash n}^{u'},\tag{37}$$

which is the desired expectation in (20).

Furthermore, according to the moment-matching method we obtain the covariance of (19) as [29, p. 106]

$$\begin{aligned}&\mathbf{S}_n(\mathbf{x}_n^u)=\\ &\sum_{\{\theta^u\}_{u=1}^U}\sum_{\{d_n^u\}_{u=1}^U}\prod_{u=1}^U\mu_{\theta^u\to g_n}(\theta^u)\prod_{u=1}^U\mu_{d_n^u\to g_n}(d_n^u)\\ &\times\left[\sum_{u'\neq u}\theta^{u'}\mathbf{H}_n^{u'}(d_n^{u'})\mathbf{P}_{n\backslash n}^{u'}\mathbf{H}_n^{u'}(d_n^{u'})^H+\mathbf{R}\right.\\ &+\left(\theta^u\mathbf{H}_n^u(d_n^u)\mathbf{x}_n^u+\sum_{u'\neq u}\theta^{u'}\mathbf{H}_n^{u'}(d_n^{u'})\hat{\mathbf{x}}_{n\backslash n}^{u'}-\mathbf{m}_n(\mathbf{x}_n^u)\right)\\ &\left.\times\left(\theta^u\mathbf{H}_n^u(d_n^u)\mathbf{x}_n^u+\sum_{u'\neq u}\theta^{u'}\mathbf{H}_n^{u'}(d_n^{u'})\hat{\mathbf{x}}_{n\backslash n}^{u'}-\mathbf{m}_n(\mathbf{x}_n^u)\right)^H\right].\end{aligned}$$

Plugging (37) into the previous expression and expanding the first term in the bracket using (36), we obtain

$$\begin{aligned}&.\mathbf{S}_n(\mathbf{x}_n^u)=\\ &\mathbf{R}+\sum_{u'\neq u}\Big\{\sum_{\theta^{u'}}\sum_{d_n^{u'}}\mu_{\theta^{u'}\to g_n}(\theta^{u'})\mu_{d_n^{u'}\to g_n}(d_n^{u'})\\ &\qquad\times\theta^{u'}\mathbf{H}_n^{u'}(d_n^{u'})\mathbf{P}_{n\backslash n}^{u'}\mathbf{H}_n^{u'}(d_n^{u'})^H\Big\}\\ &+\sum_{\{\theta^u\}_{u=1}^U}\sum_{\{d_n^u\}_{u=1}^U}\prod_{u=1}^U\mu_{\theta^u\to g_n}(\theta^u)\prod_{u=1}^U\mu_{d_n^u\to g_n}(d_n^u)\\ &\times\left((\theta^u\mathbf{H}_n^u(d_n^u)-\hat{\mathbf{H}}_n^u)\mathbf{x}_n^u+\sum_{u'\neq u}(\theta^{u'}\mathbf{H}_n^{u'}(d_n^{u'})-\hat{\mathbf{H}}_n^{u'})\hat{\mathbf{x}}_{n\backslash n}^{u'}\right)\\ &\times\left((\theta^u\mathbf{H}_n^u(d_n^u)-\hat{\mathbf{H}}_n^u)\mathbf{x}_n^u+\sum_{u'\neq u}(\theta^{u'}\mathbf{H}_n^{u'}(d_n^{u'})-\hat{\mathbf{H}}_n^{u'})\hat{\mathbf{x}}_{n\backslash n}^{u'}\right)^H.\end{aligned}$$

Now, all cross terms inside the last double summation vanish due to the independence of (θ^u,d_n^u) w.r.t $(\{\theta^{u'}\}_{u'\neq u},\{d_n^{u'}\}_{u'\neq u})$, so that

$$\begin{aligned}&\mathbf{S}_n(\mathbf{x}_n^u)=\\ &\sum_{\theta^u}\sum_{d_n^u}\mu_{\theta^u\to g_n}(\theta^u)\mu_{d_n^u\to g_n}(d_n^u)\\ &\qquad\times(\theta^u\mathbf{H}_n^u(d_n^u)-\hat{\mathbf{H}}_n^u)\mathbf{x}_n^u\mathbf{x}_n^{uH}(\theta^u\mathbf{H}_n^u(d_n^u)-\hat{\mathbf{H}}_n^u)^H\\ &+\sum_{u'\neq u}\Big\{\sum_{\theta^{u'}}\sum_{d_n^{u'}}\mu_{\theta^{u'}\to g_n}(\theta^{u'})\mu_{d_n^{u'}\to g_n}(d_n^{u'})\\ &\qquad\times\theta^{u'}\mathbf{H}_n^{u'}(d_n^{u'})\mathbf{P}_{n\backslash n}^{u'}\mathbf{H}_n^{u'}(d_n^{u'})^H\Big\}\\ &+\sum_{\{\theta^{u'}\}_{u'\neq u}}\sum_{\{d_n^{u'}\}_{u'\neq u}}\prod_{u'\neq u}\mu_{\theta^{u'}\to g_n}(\theta^{u'})\prod_{u'\neq u}\mu_{d_n^{u'}\to g_n}(d_n^{u'})\\ &\qquad\times\left(\sum_{u'\neq u}(\theta^{u'}\mathbf{H}_n^{u'}(d_n^{u'})-\hat{\mathbf{H}}_n^{u'})\hat{\mathbf{x}}_{n\backslash n}^{u'}\right)\\ &\qquad\times\left(\sum_{u'\neq u}(\theta^{u'}\mathbf{H}_n^{u'}(d_n^{u'})-\hat{\mathbf{H}}_n^{u'})\hat{\mathbf{x}}_{n\backslash n}^{u'}\right)^H\\ &+\mathbf{R}.\end{aligned}\tag{38}$$

It follows that $E[\mathbf{S}_n(\mathbf{x}_n^u)]=\int\mathbf{S}_n(\mathbf{x}_n^u)p(\mathbf{x}_n^u)d\mathbf{x}_n^u=\hat{\mathbf{D}}_n^u+\sum_{u'\neq u}\mathbf{I}_n^{u'}+\mathbf{R}$, as desired in (20). Indeed in (38), after aver-

aging out $\mathbf{x}_n^u$ using the prior (2), the first double summation is the u-th user's desired signal covariance $\hat{\mathbf{D}}_n^u$ (see (21)). Also, after some algebra the remaining summations in (38) are equal to $\sum_{u' \neq u} \mathbf{I}_n^{u'}$, where $\mathbf{I}_n^{u'}$ denotes the covariance of the MUI originating from the u'-th user (see (16)).

REFERENCES

[1] A.M. Akhtar, X. Wang and L. Hanzo, "Synergetic spectrum sharing in 5G HetNets: A harmonized SDN-enabled approach," *IEEE Comm. Mag.*, vol. 54, no. 1, pp. 40-47, Jan. 2016.

[2] Z. Zhang, X. Chai, K. Long, A.V. Vasilakos and L. Hanzo, "Full duplex techniques for 5G networks: Self-interference cancellation, protocol design, and relay selection," *IEEE Comm. Mag.*, vol. 53, no. 5, pp. 128-137, May 2015.

[3] F.F. Digham, M.S. Alouini and M.K. Simon, "On the energy detection of unknown signals over fading channels," *IEEE Trans. Commun.*, vol. 55, no. 1, pp. 21-24, Jan. 2007.

[4] V. Kuppusamy and R. Mahapatra, "Primary user detection in OFDM based MIMO cognitive radio," *Proc 3rd international conference on cognitive radio oriented wireless networks and communications (CrownCom 2008)*, pp. 1-5, Singapore, Singapore, May 2008.

[5] J. Ylioinas and M. Juntti, "Iterative joint detection, decoding, and channel estimation in turbo-coded MIMO-OFDM," *IEEE Trans. Veh. Technol.*, vol. 58, no. 4, pp. 1784-1796, May 2009.

[6] C. Knievel, P.A. Hoeher, A. Tyrrell and G. Auer, "Multi-dimensional graph-based soft iterative receiver for MIMO-OFDM," *IEEE Trans. Commun.*, vol. 60, no. 6, pp. 1599-1606, June 2012.

[7] M. Ruan, M.C. Reed, and Z. Shi, "Successive multiuser detection and interference cancelation for contention based OFDMA ranging channel," *IEEE Trans. Wireless Commun.*, vol. 9, no. 2, pp. 481-487, Feb. 2010.

[8] Q. Wang and G. Ren, "Iterative maximum likelihood detection for initial ranging process in 802.16 OFDMA systems," *IEEE Trans. Wireless Commun.*, vol. 14, no. 5, pp. 2778-2787, May 2015.

[9] B. Lu and X. Wang, "Iterative receivers for multiuser space-time coding systems," *IEEE J. Sel. Areas Commun.*, vol. 18, no. 11, pp. 2322-2335, Nov. 2000.

[10] S. Yatawatta and A.P. Petropulu, "Blind channel estimation in MIMO OFDM systems with multiuser interference," *IEEE Trans. Sig. Proc.*, vol. 54, no. 3, pp. 1054-1068, March 2006.

[11] P. Salvo Rossi and R.R. Müller, "Joint twofold-iterative channel estimation and multiuser detection for MIMO-OFDM systems," *IEEE Trans. Wireless Commun.*, vol. 7, no. 11, pp. 4719-4729, Nov. 2008.

[12] P. Hammarberg, F. Rusek and O. Edfors, "Iterative receivers with channel estimation for multi-user MIMO-OFDM: complexity and performance," *EURASIP J. Wireless Comm. Netw.*, pp. 1-17, Mar. 2012.

[13] M. Marey and O.A. Dobre, "Iterative receiver design for uplink OFDMA cooperative Systems," *IEEE Trans. Broadcast.*, vol. 62, no. 4, pp. 936-947, Dec. 2016.

[14] T. Wang and S.C. Liew, "Frequency-asynchronous multiuser joint channel-parameter estimation, CFO compensation, and channel decoding," *IEEE Trans. Veh. Technol.*, vol. 65, no. 12, pp. 9732-9746, Dec. 2016.

[15] P. Botsinis, D. Alanis, Z. Babar, S.X. Ng and L. Hanzo, "Joint quantum-assisted channel estimation and data detection," *IEEE Access*, vol. 4, pp. 7658-7681, 2016.

[16] X. Wu and Q. Yin, "Uplink vector channel estimation in ISI-corrupted MC-CDMA systems with multiple antennas," *Proc. IEEE Int. Conf. Acoustics, Speech, and Signal Processing*, vol. 3, pp. 2765-2768, Orlando, FL, May 2002.

[17] H. Zhu and G.B. Giannakis, "Exploiting sparse user activity in multiuser detection," *IEEE Trans. Commun.*, vol. 59, no. 2, pp. 454-465, Feb. 2011.

[18] B. Wang, L. Dai, T. Mir and Z. Wang, "Joint user activity and data detection based on structured compressive sensing for NOMA," *IEEE Comm. Lett.*, vol. 20, no. 7, pp. 1473-1476, Jul. 2016.

[19] F. Monsees, M. Woltering, C. Bockelmann and A. Dekorsy, "Compressive sensing multi-user detection for multicarrier systems in sporadic machine type communication," *Proc. IEEE Vehicular Technology Conference (IEEE VTC 2015 Spring)*, pp. 1-5, Glasgow, UK, May 2015,

[20] C. Bockelmann, "Iterative soft interference cancellation for sparse BPSK signals," *IEEE Comm. Lett.*, vol. 19, no. 5, pp. 855-858, May 2015.

[21] F.R. Kschischang, B.J. Frey and H.-A. Loeliger, "Factor graphs and the sum-product algorithm ," *IEEE Trans. Information Theory*, vol. 47, no. 2, pp. 498-519, Feb. 2001.

[22] H.-A. Loeliger, "An introduction to factor graphs," *IEEE Sig. Proc. Mag.*, vol. 21, no. 1, pp. 28-41, Jan. 2004.

[23] D.M. Malioutov, J.K. Johnson and A.S. Willsky, "Walk-sums and belief propagation in Gaussian graphical models," *The Journal of Machine Learning Research*, vol. 7, pp. 2031-2064, Oct. 2006.

[24] D. Bickson and D. Dolev, O. Shental, P.H. Siegel and J.K. Wolf, "Gaussian belief propagation based multiuser detection," *Proc. ISIT 08*, pp. 1878-1882, Toronto, Canada, Jul. 2008.

[25] J.J. van de Beek, P.O. Borjesson, M.L. Boucheret, D. Landstrom, J.M. Arenas, P. Odling, C. Ostberg, M. Wahlqvist, and S.K. Wilson, "A time and frequency synchronization scheme for multiuser OFDM," *IEEE J. Select. Areas Commun.*, vol. 17, no. 11, pp. 1900-1914, Nov. 1999.

[26] P. Bello, "Characterization of randomly time-variant linear channels," *IEEE Trans. Comm. Syst.*, vol. 11, no. 4, pp. 360-393, Dec. 1963.

[27] X. Li, A. Chindapol and J.A. Ritcey, "Bit-interleaved coded modulation with iterative decoding and 8-PSK signaling," *IEEE Trans. Commun.*, pp. 1250-1257, vol. 50, no. 8, Aug. 2002.

[28] P. Osti, P. Lassila, S. Aalto, A. Larmo and T. Tirronen, "Analysis of PDCCH performance for M2M traffic in LTE," *IEEE Trans. Veh. Technol.*, vol. 63, no. 9, pp. 4357-4371, Nov. 2014.

[29] H. Tanizaki, *Nonlinear filters: estimation and applications*, Berlin, Germany: Springer, 1996.

[30] D.C. Fraser and J.E. Potter, "The optimum linear smoother as a combination of two optimum linear filters," *IEEE Trans. Automat. Contr.*, pp. 387-390, vol. 14, no. 4, Aug. 1969.

[31] S. ten Brink, "Convergence behavior of iteratively decoded parallel concatenated codes," *IEEE Trans. Commun.*, vol. 49, no. 10, pp. 1727-1737, Oct. 2001.

[32] D.P. Shepherd, Z. Shi, M. Anderson and M.C. Reed, "EXIT chart analysis of an iterative receiver with channel estimation," *Proc. IEEE Global Telecommunications Conference (IEEE Globecom 2007)*, pp. 4010-4014, Washington, DC, USA, Nov. 2007.

[33] F. Brannstrom, L.K. Rasmussen and A.J. Grant, "Convergence analysis and optimal scheduling for multiple concatenated codes," *IEEE Trans. Information Theory*, vol. 51, no. 9, pp. 3354-3364, Sept. 2005.

[34] L. Dai, B. Wang, Y. Yuan, S. Han, C.-L. I, and Z. Wang, "Non-orthogonal multiple access for 5G: solutions, challenges, opportunities, and future Research trends," *IEEE Comm. Mag.*, vol. 53, no. 9, pp. 74-81, Sept. 2015.

Frederic Lehmann received the E.E. degree and the M.S.E.E. degree from ENSERG, France, in 1998. In 2002, he received the PhD in Electrical Engineering from the National Polytechnical Institute, Grenoble (INPG), France. He worked as a Research Engineer with STMicroelectronics from 1999 to 2002. From 2003 to 2004 he was a Post-doctoral Researcher at LAAS (Laboratory for Analysis and Architecture of Systems), CNRS, Toulouse, France. Currently, he is an Assistant Professor at Institut MINES-TELECOM, Telecom SudParis, Evry, France. His main research interests are in the area of communication theory, non-linear signal processing and statistical image processing.